Eur Biophys J (2011) 40:761–774
DOI 10.1007/s00249-011-0689-0

ORIGINAL PAPER

The DFPase from *Loligo vulgaris* in sugar surfactant-based bicontinuous microemulsions: structure, dynamics, and enzyme activity

Stefan Wellert · Brigtte Tiersch · Joachim Koetz · André Richardt · Alain Lapp · Olaf Holderer · Jürgen Gäb · Marc-Michael Blum · Christoph Schulreich · Ralf Stehle · Thomas Hellweg

Received: 29 June 2010 / Revised: 11 February 2011 / Accepted: 17 February 2011 / Published online: 17 March 2011

Abstract The enzyme diisopropyl fluorophosphatase (DFPase) from the squid *Loligo vulgaris* is of great interest because of its ability to catalyze the hydrolysis of highly toxic organophosphates. In this work, the enzyme structure in solution (native state) was studied by use of different scattering methods. The results are compared with those from hydrodynamic model calculations based on the DFPase crystal structure. Bicontinuous microemulsions made of sugar surfactants are discussed as host systems for the DFPase. The microemulsion remains stable in the presence of the enzyme, which is shown by means of scattering experiments. Moreover, activity assays reveal that the DFPase still has high activity in this complex reaction medium. To complement the scattering experiments cryo-SEM was also employed to study the microemulsion structure.

Keywords Dynamic light scattering · Neutron spin echo · Microemulsion · Enzyme catalysis · SANS · Protein structure

Introduction

The substrates of enzymes are often insoluble in water. Protein molecules, however, are usually hydrophilic.

S. Wellert (✉)
TU Berlin, Institut für Chemie, Stranski-Laboratorium für Physikalische und Theoretische Chemie,
Straße des 17.Juni 124, 10623 Berlin, Germany
e-mail: s.wellert@tu-berlin.de

B. Tiersch · J. Koetz
Institut für Chemie, Universität Potsdam, 14469 Potsdam, Germany

A. Richardt
Wehrwissenschaftliches Institut für Schutztechnologien–ABC-Schutz, Humboldtstraße 29633, Munster, Germany

A. Lapp
Laboratoire Léon Brillouin, C.E.A.-C.E.N. Saclay, 91191 Gif-sur-Yvette Cedex, France

O. Holderer
Jülich Center for Neutron Scattering, FRM II Garching, Lichtenbergstr. 1, 85747 Garching, Germany

J. Gäb · M.-M. Blum
Blum-Scientific Services, Cecilienstrasse 3, 22301 Hamburg, Germany

R. Stehle
Soft Matter und Funktionale Materialien, Helmholtz-Zentrum Berlin für Materialien und Energie, Hahn-Meitner Platz1, 14109 Berlin, Germany

C. Schulreich · T. Hellweg (✉)
Physikalische und Biophysikalische Chemie, Universitätsstr. 25, 33615 Bielefeld, Germany
e-mail: thomas.hellweg@uni-bielefeld.de

Present Address:
J. Gäb
Institute of Pharmaceutical Chemistry, Phillipps University Marburg, 35032 Marburg, Germany

Present Address:
M.-M. Blum
Bioscience Division, Los Alamos National Laboratory, PO Box 1663, Mailstop G758, Los Alamos, NM 87545, USA

Nature overcomes this problem by compartmentalization of the cytoplasm and by generating huge interfaces between polar and apolar regions inside the different relevant organelles.

For biotechnological applications an approach mimicking this compartment formation has already been successfully employed. This is the use of so-called microemulsions. Microemulsions are thermodynamically stable mixtures of water and oil forming nanoscale compartments stabilized by surfactants and sometimes co-surfactants. Since the 1980s, these structures have been the subject of numerous studies exploring, for example, phase behavior, microscopic structure and the effect of the composition of the amphiphilic film (Kahlweit and Strey 1985; Strey 1994, 1996; Iwanaga et al. 1998; Burauer et al. 1999; Hellweg and von Klitzing 2000; Hellweg 2002). The existence of different phase structures can be thermodynamically explained by using the Helfrich Hamiltonian (Helfrich 1973) for the elastic free energy F_{el}, which describes the curvature and shape fluctuations of the surfactant interface in terms of mechanical and topological constants (Milner and Safran 1987; Farago et al. 1990; Hirai et al. 1999; Safran 1999; Hellweg et al. 2001; Kawabata et al. 2007).

In previous work, a series of enzymes which remain structurally stable and catalytically active when confined to the aqueous domain of a microemulsion has already been found (Lee and Biellmann 1987; Larsson et al. 1991; Komves et al. 1994; Stamatis et al. 1999; Biswas et al. 2008).

This observation, the nanoscale compartments, and the enormous size of the internal interface, of the order of m^2/ml, makes microemulsions a promising carrier for the enzymatic decontamination of toxic lipophilic organophosphate compounds. In this concept the microemulsion solubilizes the lipophilic compound in the oil phase and the active enzyme inside the aqueous phase. Both are separated by the surfactant film and either an interfacial reaction or passage of the organophosphate because of its residual solubility in aqueous media mediates the decontamination reaction.

However, some of the surfactants used for microemulsion design denature enzymes. Therefore, in this work we present a sugar surfactant-based "mild" microemulsion, which does not harm protein structure and function. Sugar surfactants are often used in the crystallization of proteins and are known to leave the structure unchanged (Zouni et al. 2005). Moreover, they are prepared from renewable resources and have low health and other risks (Holmberg 2001; Stubenrauch 2001).

Enzymes that catalyze the hydrolysis of highly toxic organophosphorus (OP) compounds, which act as irreversible inhibitors of acetylcholinesterase, have been the subject of intense research in recent years. Hydrolysis leads to detoxification of these OP compounds, which are used as chemical warfare agents (nerve agents) or pesticides (Richardt and Blum 2008).

The enzyme diisopropyl fluorophosphatase (DFPase) from the squid *Loligo vulgaris* efficiently detoxifies diisopropyl fluorophosphate (DFP) and G-type nerve agents, for example tabun (GA), sarin (GB), soman (GD), and cyclosarin (GF) (Hoskin 1971; Hoskin and Roush 1982; Scharff et al. 2001). During the course of the reaction the phosphorus–fluorine bond (or the bond between phosphorus and the cyano group in GA) is cleaved, resulting in a phosphate or phosphonate and a fluoride ion. DFPase has remarkable thermal stability and tolerance toward organic solvents.

For example, it has been observed that DFPase remains stable for six hours in aqueous mixtures with up to 50% THF and 30% ACN. However, the hydrolysis requires the presence of water, and an organic solvent is necessary for dissolution of the lipophilic toxic organophosphates.

DFPase can be expressed in bulk and is, therefore, a prime candidate for use in enzymatic decontamination.

In addition to this, DFPase is a structurally well characterized protein with an atomic resolution X-ray structure (PDB: 1PJX, 0.85 Å) (Koepke et al. 2003) and even a neutron diffraction structure (PDB: 3BYC) (Blum et al. 2009) available (Fig. 1). On the basis of structural, kinetic, and isotope labeling data, the reaction mechanism for DFPase has been elucidated (Blum et al. 2006). DFPase can be used in bicontinuous microemulsions where it remains catalytically active, as was recently shown by the use of NMR spectroscopy (Gäb et al. 2010). However, deviations of the structure of the enzyme in solution and potential interactions of the protein with the microemulsion's interface could not be derived from the NMR data. Therefore, the objectives of this study were twofold. First, the structure of the enzyme in its native state in solution was investigated by use of dynamic light scattering (DLS), small angle neutron scattering (SANS), and neutron spin-echo spectroscopy (NSE). These measurements and related

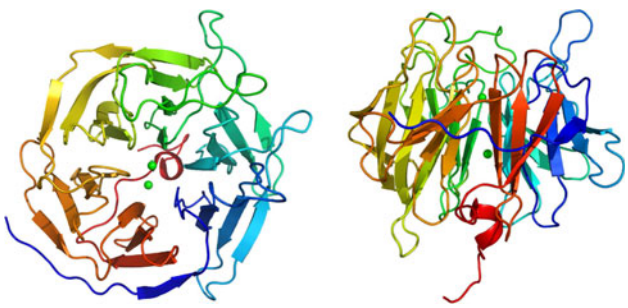

Fig. 1 Tertiary structure of diisopropyl fluorophosphatase (DFPase) in *top* and *side* views

hydrodynamic model calculations enable comparison of the crystalline and solution structures (Garcia de la Torre et al. 2000). The second objective of this contribution was to explore the structure and dynamics of the microemulsion in the absence and presence of the DFPase molecule. These investigations were performed by use of different scattering techniques. In this context, neutron spin-echo spectroscopy (NSE) is of special importance, because NSE data can be used to compute the bending elastic constant of the amphiphilic interface. The bending elasticity of the surfactant film would be affected by all the substances incorporated into the interface.

Materials and methods

Materials

Cyclohexane and pentanol (purity >99%) were purchased from Sigma–Aldrich. Cyclohexane D12 (isotopic purity ≥99.5%, residual water content ≤0.02) and D_2O (purity ≥98%, isotopic purity ≥99.9%) were purchased from Eurisotop, France. The sugar surfactant $C_{8/10}G_{1.3}$ (Glucopon 220; Cognis, Germany) was technical grade aqueous stock solution. The water content, 43%, was determined by Karl–Fischer titration and is taken into account in sample preparation. Moreover, for replacement of water by D_2O in the neutron-scattering experiments the water was removed from the surfactant solution by freeze drying the stock solution. The residual content was less than 1%. For the studies of the phase behavior, demineralized water from a MilliQ system (Millipore) was used. The nerve agent sarin (GB) was made available by the German Ministry of Defense and experiments were carried out at the Bundeswehr Institute of Pharmacology and Toxicology in Munich, Germany, in accordance with the Chemical Weapons Convention.

DFPase

His-tagged DFPase was expressed in *E. coli* BL21 cells and purified by metal chelate affinity chromatography on Ni-NTA resin and by cation-exchange chromatography on Q-Sepharose HP, by the method of Hartleib and Rüterjans (2001). Briefly, DFPase was over-expressed in *E. coli* pKKHisND. Cells were sonicated, and the supernatant was applied to a Ni-NTA column in 3 mM imidazole, 500 mM NaCl, 10 mM Tris (pH 7.5), and 2 mM $CaCl_2$. The target protein was eluted with 300 mM imidazole. The His tag was removed by thrombin cleavage overnight and dialyzed against 10 mM Tris buffer (pH 7.5, 2 mM $CaCl_2$) to remove the imidazole, followed by rechromatography on an Ni-NTA column. After another overnight dialysis the flow-through fraction was applied to a Q-Sepharose HP column, and a gradient of 0–500 mM NaCl was run. The target eluted at 50 mM NaCl. For all scattering experiments deuterated buffer was used.

Methods

Studies of the microemulsion phase behavior

The phase behavior of sugar surfactant-based systems is less sensitive to temperature variations than systems containing surfactants of the C_iE_j-type (Strey 1994, 1996; Stubenrauch 2001; Aveyard et al. 1998; Stradner et al. 2000). Therefore, in sugar surfactant-based systems the addition of short or medium chain alcohols is used to tune the curvature of the amphiphilic film and to control the phase behavior (Stubenrauch 2001; Stradner et al. 2000; Möller et al. 1998; Glatter et al. 2001; Wellert et al. 2008). In our work the phase behavior of the quaternary mixture cyclohexane–water–$C_{8/10}G_{1.3}$–pentanol was determined by using a cut (Kahlweit and Strey 1985; Strey 1996) through the phase tetrahedron at a constant oil-to-water ratio $\alpha = 0.5$ as a function of the surfactant weight fraction, γ, in the water-oil-surfactant mixture and the overall alcohol weight fraction, δ (Kahlweit and Strey 1985). For a series of samples the alcohol concentration was gradually increased, starting from a ternary mixture at $\delta = 0$. After each step the phase behavior was determined by visual inspection of the equilibrated samples. Because the phase behavior in a sugar surfactant-based system is of low temperature sensitivity, only samples very close to phase boundaries were equilibrated in thermostated baths. Static birefringence observed with crossed polarizers was used to identify the location of the lamellar phase. More details about phase behavior studies of sugar surfactant-based systems can be found elsewhere (Stubenrauch 2001; Wellert et al. 2008).

Cryo scanning electron microscopy (Cryo-SEM)

The structure of the sugar surfactant-based microemulsion was examined by using a cryo-high-resolution scanning electron microscope S-4800 from Hitachi, equipped with a field emission gun. The microemulsion sample was cooled by plunging it into nitrogen slush at atmospheric pressure. Subsequently, the samples were freeze-fractured at −180°C, etched for 60 s at −98°C, and sputtered with platinum in the GATAN Alto 2500 cryo-preparation chamber and then transferred into the cryo-SEM.

Measuring DFPase activity

Because of safety regulations the nerve agent GB was handled in a 1% (*m*/*v*, 71 mM) stock solution in

cyclohexane. The microemulsion samples containing GB were prepared as follows. Glucopon 220 was dissolved in D_2O buffered with 50 mM TRIS at pD 7.5. As the surfactant was slightly basic the pD was adjusted to pD 7.5 with DCl. The TRIS buffer was necessary to maintain the pD during the hydrolysis of the nerve agent, because protons are released in this reaction. 1-Pentanol was added and the mixture was split into two samples.

Both samples were spiked with 100 μL GB stock solution just before starting the experiment. Cyclohexane was then added to 1.0 g, resulting in an optically clear microemulsion. One sample was spiked with 2.5 μL (3.025 mg/ml) wildtype DFPase whereas the other sample without the enzyme was used to determine autohydrolysis of the nerve agent. The two samples were measured by use of the nondecoupled ^{1}H–^{31}P HSCQ NMR technique of Gäb et al. (2010). The reaction was followed over a period of 100 min and every data point was composed of 16 single FIDs. The peak area of the developing doublet signal at ca. 1.3 ppm (methyl protons directly bound to phosphorus), indicating the appearance of the hydrolysis product isopropyl methylphosphonate (IMPA), was used as a measure of the hydrolytic cleavage of the nerve agent GB; this is more accurate than the vanishing doublet of doublets signal of GB that arises because of additional coupling with the fluorine and is therefore more difficult to integrate.

Small angle neutron scattering

All SANS measurements were done using the PAXY instrument at the Laboratoire Léon Brillouin (Saclay, France). The used wavelength, λ, of 6 Å was obtained by means of a mechanical velocity selector and three sample to detector distances of 1.06, 3.06, and 6.76 m were used. Using the wavelength and the solid angle "seen" by the detector at different sample to detector distances, the magnitude of the scattering vector q is obtained according to:

$$q = \frac{4\pi}{\lambda}\sin\frac{\theta}{2},$$

where θ is the scattering angle.

The path length in the quartz sample cells was 2 mm for the DFPase samples and 1 mm for the microemulsion samples. Enzyme solutions of 1 mg/ml (A), 5 mg/ml (B), and 10 mg/ml (C) were measured (Table 1). Microemulsion samples of identical γ, δ, and α but different aqueous phase were measured in bulk contrast using pure D_2O (sample D), deuterated buffer (E), and an enzyme solution of 10 mg/ml (F) (Table 2); all other components were used in their protonated form.

Table 1 Enzyme volume fraction in aqueous solution Φ, radius R, and polydispersity index P resulting from SANS measurements of three DFPase samples in buffered deuterated solution

Sample	c (mg/ml)	Φ	R (Å)	P
A	1.0	0.0011	20.36	0.087
B	5.0	0.0056	19.74	0.077
C	10.0	0.011	20.16	0.072

Table 2 Composition of samples D, E, and F and results of bulk contrast SANS measurements

Sample	Aqueous phase	α	γ	δ	d (Å)	ξ (Å)
D	D_2O	0.5	0.2151	0.0606	155.36	69.28
E	Buffer	0.5	0.2146	0.0599	157.17	69.57
F	DFPase solution	0.5	0.2146	0.0600	155.71	64.99

Mean domain size d, and correlation length ξ were obtained by Teubner–Strey analysis of the SANS data

The initial data treatment and the absolute intensity calibration were done with the software and methods developed by the LLB (Cotton 1991; Brûlet et al. 2007).

DLS measurements

For the DLS measurements a standard goniometer arrangement with pinhole collimation (ALV, Langen, Germany), an Ar^{+}-Ion Laser (model 2017; Spectra Physics, USA) with a nominal maximum power of 1 W at $\lambda = 514.5$ nm and a multiple-τ correlator ALV-5000/E (ALV, Langen, Germany) was used. Impurities were separated from the enzyme samples by filtration with an Anotop filter of pore size 100 nm before transfer to dust-free cylindrical Hellma quartz cells of 1 cm outer diameter. The measurements were done at 15°C to reduce potential enzyme degradation during the measurements. From the experimentally determined normalized intensity time correlation function $g^2(\tau)$ the normalized time autocorrelation function $g^1(\tau)$ of the electrical field was obtained by use of the Siegert relationship.

The data were analyzed using the inverse Laplace transformation of the field correlation function by means of the software CONTIN (Provencher 1982a, b).

Neutron spin-echo spectroscopy

Neutron spin-echo spectroscopy (NSE) provides access to the dynamics on the nanometer length scale and to relaxations taking place in the range from 100 ps to 0.5 μs. The dynamics of shape fluctuations of the surfactant interface in droplet and bicontinuous microemulsions can be studied directly without perturbation of the sample (Hellweg et al. 2000, 2001; Kawabata et al. 2007; Mihailescu et al. 2001; Endo et al. 2001; Holderer et al. 2005; Huang et al. 1987; Farago et al. 1995; Farago and Gradzielski 2001).

Furthermore, the dynamics of biological systems is also accessible by NSE. The membrane undulation of lipid vesicles can be directly observed (Arriaga et al. 2009a, b, 2010). The center of mass diffusion of proteins, also, has already been studied by use of NSE (Koeper and Bellissent-Funel 2000; Bu et al. 2005; Doster and Longeville 2007; Wood et al. 2008; Coeur and Longeville 2008). A recent approach uses NSE measurements in combination with normal mode analysis to reveal coupled domain motions in proteins (Bu et al. 2005; Biehl et al. 2008). Additionally, first results on the dynamics of proteins confined in a reverse droplet microemulsions studied with NSE have been reported (Hirai et al. 2002).

The NSE experiments were carried out using the J-NSE instrument (Monkenbusch 1997; Monkenbusch et al. 1997) at the FRMII neutron source in Garching, Germany. The enzyme solutions B and C (Table 1) were measured at five q values from $q = 0.05$ Å^{-1} to $q = 0.18$ Å^{-1}. The path length in the Hellma quartz cells was 2 mm. All samples were measured at 15°C. The microemulsion samples were prepared in film contrast using deuterated cyclohexane, deuterated buffer (K), and enzyme concentrations of 5 mg/ml (L) and 10 mg/ml (M) (Table 2). Pentanol and surfactant were used in their protonated forms. In the so-called film contrast all of the sample is deuterated except the surfactant interface. In neutron-scattering experiments only the protonated part gives rise to coherent scattering and is therefore seen in the experiment.

The samples were measured at six q values in the momentum transfer range from $q = 0.05$ Å^{-1} to $q = 0.21$ Å^{-1} using neutron wavelengths of 12, 10, and 8 Å.

Hydrodynamic model calculations

Proteins have a rather well defined rigid structure compared with synthetic polymers and their transport properties can therefore be computed using the rigid body formalism introduced by Kirkwood and Riseman (Kirkwood 1949; Riseman and Kirkwood 1950). This approach was extended by Bloomfield and Gracia de la Torre (Garcia de la Torre and Bloomfield 1977; Garcia Bernal and Garcia de la Torre 1980; Garcia de la Torre and Bloomfield 1981). Details of the technique and of the different cases in which it has been successfully applied can be found in (Garcia de la Torre et al. 2000).

This technique enables the crystal structure of a protein to be compared with the "native" structure in solution (Hellweg et al. 1997), and detection of possible significant differences.

In this study we used neutron diffraction and X-ray data for the DFPase molecule (Blum et al. 2009) (PDB code: 3BYC) as a basis for the hydrodynamic model calculations. The model used only contains the α-C atoms as coordinates for the frictional centers (beads) and different radii were used to calculate the theoretical translational diffusion coefficient for the "dry" and the hydrated protein.

The calculations were done using the Fortran software Hydro provided by J. Garcia de la Torre employing only the Oseen hydrodynamic interaction tensor (Garcia de la Torre et al. 2000).

Results and discussion

DFPase in solution

DLS results

The DLS measurements were carried out at 15°C and at different scattering angles. Figure 2 shows an example of the normalized intensity autocorrelation functions measured for sample B at $q = 0.023$ nm^{-1}, corresponding to a detection angle of 90°. The resulting relaxation rate distributions are also shown in Fig. 2. The inset shows three examples of the relaxation rate distributions measured at three scattering angles (■ q = 0.0163 nm^{-1} (60°), • q = 0.0198 nm^{-1} (75°), ▲ q = 0.023 nm^{-1} (90°)). Figure 3 shows the resulting relaxation rates Γ as a function of q^2. As expected for pure translational center of mass diffusion the relaxation rates Γ obtained for the DFPase molecules in heavy water exhibit a linear dispersion with regard to q^2. The mutual diffusion coefficient D_m determined from the slope is $D_m = (6.52 \pm 0.21) \times 10^{-7}$ cm^2/s for the enzyme in deuterated buffer solution. From the Stokes–Einstein equation:

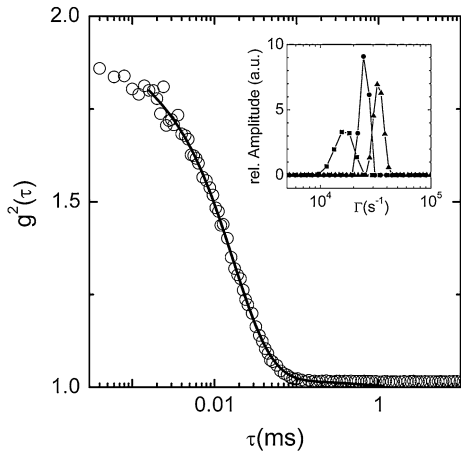

Fig. 2 Example of a normalized intensity correlation function $g^2(\tau)$, measured at $q = 0.023$ nm^{-1} (scattering angle 90°). The *inset* shows three examples of the relaxation rate distributions obtained from inverse Laplace transformation at three angles (*filled squares*, $q = 0.0163$ nm^{-1} (90°); *filled circles*, $q = 0.0198$ nm^{-1} (75°); *filled triangles*, $q = 0.023$ nm^{-1} (90°))

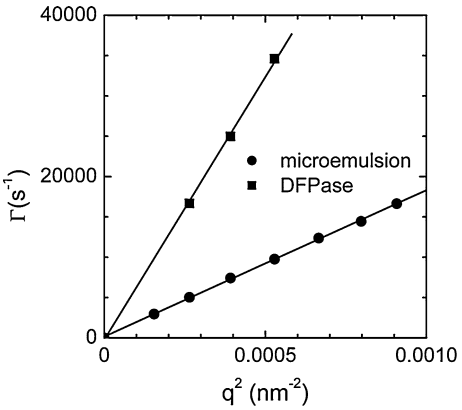

Fig. 3 Mean relaxation rate as a function of q^2 for DFPase sample B at 15°C (*filled squares*) and a bicontinuous microemulsion sample of the investigated system (D) measured at 20°C (*filled circles*). The *solid lines* are fits according to $\Gamma = D_m q^2$

$$R_{\mathrm{h}} = \frac{k_B T}{6\pi\eta D_m} \tag{1}$$

a hydrodynamic radius R_{h} of 2.34 nm is obtained for the enzyme solution using a solvent viscosity of $\eta = 1.387$ mPas (heavy water at 288.15 K).

Hydrodynamic model calculations

On the basis of the crystal structure of the DFPase (Blum et al. 2009) (Fig. 1) a simplified model of the protein is made. The model contains the coordinates of the 312 α-C atoms. These are used as coordinates for the bead model. The calculations were done using the Oseen approximation for the hydrodynamic interaction. In the first calculation the bead radius used was set to 0.36 nm. This bead radius has been used previously (Hellweg et al. 1997). Based on this value a translational diffusion coefficient in D_2O of 6.98×10^{-7} cm^2/s is obtained at $T = 288.15$ K. This very simple model, which does not account for hydration, already leads to a computed translational diffusion coefficient that is close to the experimental value of $D_{\mathrm{m}} = (6.52 \pm 0.21) \times 10^{-7}$ cm^2/s.

It is known that at least about one hydration shell is nearly immobilized on the surface of proteins and therefore the model has to be modified to account for this. In previous work we have already shown that the hydration can be simply modeled by increasing the bead radius by approximately 0.28 nm, which corresponds to the approximate diameter of a water molecule (Hellweg et al. 1997). Hence, we also used this approach in the present case also, leading to a radius of 0.64 nm for the frictional centers. Doing so, a translational diffusion coefficient of $D = 6.55 \times 10^{-7}$ cm^2/s is computed using the Oseen tensor. Within the precision of the experiment and the model calculations this value is identical with the experimental result. Hence, it is straightforward to conclude that the crystal structure of the DFPase molecule is very close to the "native" structure in solution. The radius of gyration obtained from this last model is 1.83 nm. The model without the hydration shell has an R_{g} of about 1.78 nm.

Estimates of the anisotropy of the DFPase From the friction coefficient $f = 6\pi\eta R$ the anisotropy of the structure can be estimated if the experimentally measured hydrodynamic radius is compared with a theoretical value according to:

$$\frac{f}{f_{\mathrm{theo}}} = \frac{R}{R_{\mathrm{theo}}} \tag{2}$$

Here, R_{theo} is a calculated hydrodynamic radius assuming a globular structure for the protein, given by:

$$R_{\mathrm{theo}} = \left(\frac{3Mv}{4\pi N_A}\right)^{1/3} \tag{3}$$

taking into account the molecular mass M and the mean specific volume v of the enzyme. With a molecular mass of $M = 35$ kDa and a typical value of $v = 0.73$ cm^3/g for the specific volume the theoretical hydrodynamic radius $R_{\mathrm{theo}} = 2.16$ nm (Hellweg et al. 1993). The ratio $R/R_{\mathrm{theo}} = 2.34$ nm/2.16 nm gives 1.08. The result of this estimation deviates only slightly from unity and therefore indicates that the enzyme structure in solution only marginally deviates from a globular structure.

Small-angle neutron scattering

In Fig. 4 the scattered intensity profile is depicted for the enzyme solutions (samples A, B, and C). Because of the

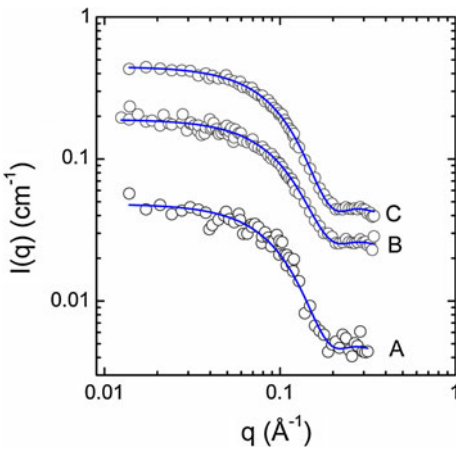

Fig. 4 SANS spectra of DFPase in buffered solution at three concentrations (*A*, 1 mg/ml; *B*, 5 mg/ml; *C*, 10 mg/ml). The curves are fitted with a hard sphere form factor with a Gaussian size distribution. Results are summarized in Table 1

lower enzyme concentration the scattering curves measured for samples A and B have rather poor statistics compared with that for sample C. However, all three curves can be analyzed in terms of a polydisperse hard-sphere form factor. In general, the scattered absolute intensity $I(q)$ is proportional to the structure factor $S(q)$ and the form factor $P(q)$ of the investigated system:

$$I(q) \propto \phi V_{part} S(q) P(q) \tag{4}$$

where ϕ is the particle number density. V_{part} is the volume of a single particle (Pedersen 1997). Because of the low enzyme concentrations in the samples $S(q) = 1$ is a good approximation for the structure factor of the DFPase solutions. The Carnahan–Starling approach enables estimation of $S(q = 0)$ (Carnahan and Starling 1969), from the volume fraction of the scatterers. The DFPase concentration in sample C corresponds to an approximate hard sphere volume fraction: Φ of 0.01 using an estimated specific volume of the DFPase of 0.73 cm^3/g. And, indeed, on the basis of this volume fraction, a value of $S(q = 0) \approx 1$ is computed, which indicates that contributions from enzyme–enzyme interactions can be neglected and the SANS curves are dominated by $P(q)$.

The SANS data of the three enzyme concentrations were analyzed with the software package SASfit (Kohlbrecher 2008). Based on the fact that the anisotropy of the DFPase molecules is very small it is straightforward to assume a polydisperse globular structure of the enzyme. Therefore, the hard sphere form factor and a polydispersity of the radius R, described by a Gaussian size distribution were used for the fit. For sample A, a radius of 20.36 Å and a polydispersity $p = 0.087$ was obtained. Analysis of curves B and C results in 19.74 Å ($p = 0.077$) and 20.16 Å ($p = 0.072$), respectively. In addition to this, an ellipsoid form factor was fitted to the data considering a small anisotropy of the DFPase molecules. Within the precision of the best fits to the data no difference in the results was observed (data not shown). Because use of an ellipsoid form factor increases the number of adjustable terms without a significant advantage in data description, the hard sphere model is more appropriate in this case.

Moreover, the radii for the enzyme obtained under the assumption of a globular structure are in good agreement with the results obtained from the DLS measurements and also with model calculations.

The polydispersity of 7–8% indicates that no observable protein aggregation occurs during the measuring time of a few hours at all three concentrations.

Using the radius of gyration computed on the basis of the SANS data and the value of the hydrodynamic radius a ρ term, defined as the ratio of these radii, of $\rho = 0.86$ is calculated. A solid sphere would give a value of ca. 0.7 (Burchard and Richtering 1989). Taking the radius of gyration obtained on the basis of the hydrodynamic bead model we obtain $\rho = 0.78$. Hence, the hard sphere model is not too bad an approximation for describing the DFPase in aqueous solution.

Neutron spin-echo measurements

Before investigating the dynamics of microemulsion samples containing the enzyme in the aqueous domain, a DFPase solution in deuterated buffer was measured with NSE to determine the contribution of the enzyme to the collective dynamics in the system. Although the dynamics of internal deformation modes are beyond the scope of this work, their effect on the measured signal must be determined, because such modes contribute to the NSE signal, as recently reported by Biehl et al. (2008).

Figure 5 shows the normalized and background corrected intermediate scattering function $S(q, \tau_{NSE})/S(q, 0)$ in a semi-logarithmic representation for sample C at representative q values ranging from $q = 0.05$ $Å^{-1}$ to $q = 0.15$ $Å^{-1}$.

The method of cumulants was used to obtain the effective diffusion coefficient D_{eff} from the experimental data (Koppel 1972; Bargeron 1974). According to the cumulant series expansion:

$$\ln \frac{S(q, \tau_{NSE})}{S(q, 0)} = -K_1 \tau_{NSE} + \frac{1}{2} K_2 \tau_{NSE}^2 - \frac{1}{3!} K_3 \tau_{NSE}^3 + \frac{1}{4!} K_4 \tau_{NSE}^4 - \cdots \tag{5}$$

the effective diffusion coefficient:

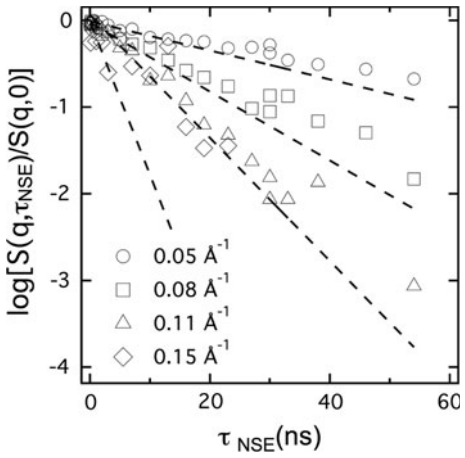

Fig. 5 Semi-logarithmic representation of the normalized intermediate scattering functions of a buffered DFPase solution in D_2O of a concentration of 10 mg/ml at different representative q values. The measurements were obtained at 15°C. The data were fitted according to the method of cumulants

$$D_{eff} = \frac{K_1}{q^2} \tag{6}$$

was calculated from the first cumulant K_1. K_1 was determined from a linear fit to $\ln[S(q, \tau_{NSE})/S(q, \tau_{NSE})]$. All higher terms in Eq. 5 were omitted and only the initial slope is determined. This is an approach frequently used in analysis of NSE data (Milner and Safran 1987; Hellweg et al. 2001; Huang et al. 1987).

In Fig. 6 the resulting effective diffusion coefficient is represented as a function of q for samples B and C.

In addition to these values the mutual diffusion coefficient measured with DLS and the diffusion coefficient obtained from the hydrodynamic model calculations are plotted as dashed and dashed–dotted lines in the same figure. Within the experimental accuracy D_{eff} compares well with the DLS results and the hydrodynamic model calculation. At $q = 0.18$ Å^{-1} an increase of the effective diffusion coefficient due to the contribution from deformation modes of the tertiary and secondary structure of the DFPase close to the form factor minimum is observed. This upturn in D_{eff} is in good agreement with recent findings by Biehl et al. (2008). The large error at this point results from the strong decrease of the scattering signal. Unfortunately, because of the low count rate it was not possible to measure the intermediate scattering function of the lower protein concentration for this q value in an acceptable time.

All three methods, DLS, NSE, and model calculations, are in excellent agreement and within the precision of the different methods identical values for the translational diffusion coefficient are found for the DFPase molecule (Fig. 1). However, NSE is obviously able to go beyond the simple diffusion measurement. This is promising for future experiments on the collective dynamics of the tertiary structure of proteins.

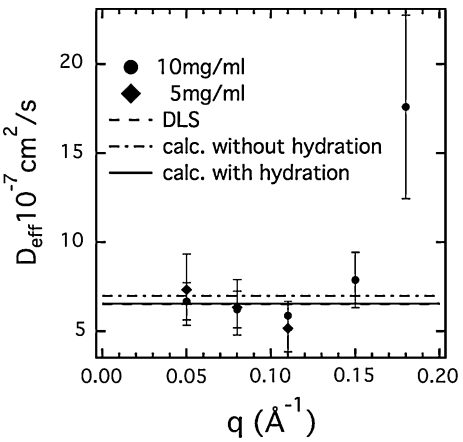

Fig. 6 Effective diffusion coefficient D_{eff} as a function of q for samples B and C. For comparison, the diffusion coefficients resulting from DLS (*dashed line*) and hydrodynamic calculations (*dashed–dotted line*) are plotted

DFPase in a bicontinuous microemulsion as reaction medium

Microemulsion phase behavior

Figure 7 shows the microemulsion phase diagram at a constant cyclohexane-to-water ratio of $\alpha = 0.5$ as a function of the $C_{8/10}G_{1.3}$ (Glucopon 220) weight fraction γ and the total pentanol weight fraction δ. The sequence and location of the individual phases resembles the well-known behavior in microemulsion forming systems based on surfactants of the C_iE_j-type described for the first time by Kahlweit et al. (1987). The three-phase body starts at $\gamma = 0.01$. At a surfactant concentration of $\gamma = 0.124$ the single-phase bicontinuous region appears. This position where four phase regions meet in one point is defined as the X-point. With increasing surfactant content above $\gamma = 0.25$ the one-phase region passes into the lamellar phase, which is separated from the single-phase region by a thin two-phase channel. The position of the phase boundaries changes only slightly when deuterated solvents are used.

Structural characterization

For the experiments described in this article a composition within the bicontinuous region with a rather large distance from the X-point was chosen. This is ensured at $\gamma = 0.21$ as can be seen in Fig. 7. Characterization of the structure at this composition point is essential. An imaging and a scattering technique were therefore chosen as two independent and complementary methods to characterize the bicontinuous structure at the chosen composition. This is described below, in the sections Cryo-SEM imaging and Structural properties by SANS.

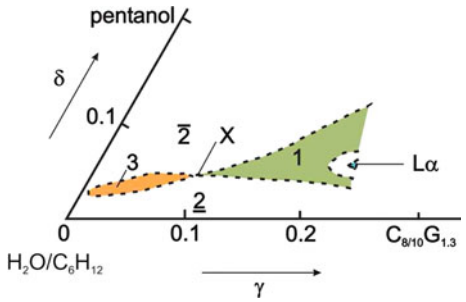

Fig. 7 Cut through the phase tetrahedron of the system cyclohexane–water–$C_{8/10}G_{1.3}$–pentanol at an oil-to-water ratio $\alpha = 0.5$. The *3* indicates the three-phase body. *1* marks the single-phase microemulsions (*green area*) starting at the X-point. Above and below the three-phase and single-phase regions the two-phase regions $\bar{2}$ and $\underline{2}$ of water-in-oil droplet phase with lower excess phase and oil-in-water droplet phase with upper excess phase were observed. More details are available elsewhere, for example (Strey 1996)

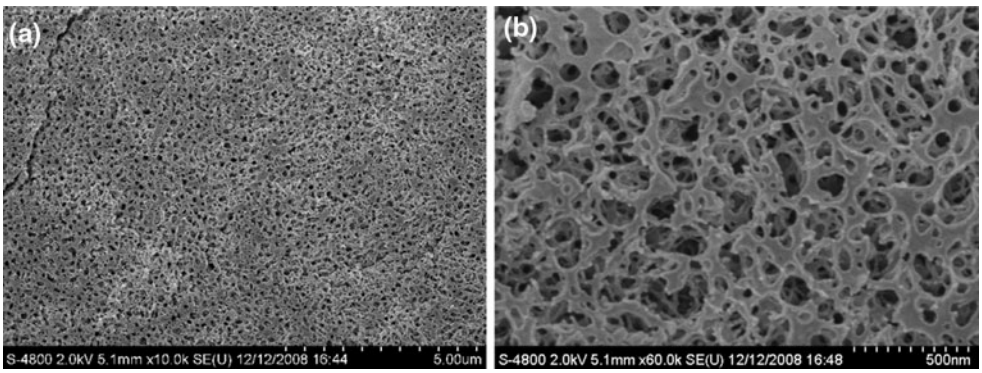

Fig. 8 Cryo-SEM micrographs at different resolution of a bicontinuous microemulsion from the green region of the phase diagram in Fig. 7

Cryo-SEM imaging

Cryo scanning electron microscopy can be successfully used for characterization of different types of microemulsions. Especially, the L_2-phase, that means water-in-oil droplets, can be visualized nicely by means of this technique, as already demonstrated in water–SDS–xylene–pentanol based microemulsions (Baier et al. 2007). In addition, it has been demonstrated that the transition from the L_2-phase to a bicontinuous sponge phase (by increasing the water content) can be identified easily by means of cryo-SEM (Lutter et al. 2009). Furthermore, freeze fracture transmission electron microscopy can be used for characterization of bicontinuous microemulsions also (Wellert et al. 2008; Jahn and Strey 1988). Recently, Rojas et al. (2009) have shown by means of cryo-SEM that a morphological change from a droplet-like to a sponge-like structure is accompanied by a structural change from an L_2-phase to a bicontinuous microemulsion phase, proved by a characteristic change of the reduced diffusion coefficients obtained by NMR spectroscopy. Our cryo-SEM micro-graphs of a sample from the bicontinuous region of the phase diagram (compare Fig. 7) show the typical morphology of a sponge-phase, in good agreement to the micro-graphs of the bicontinuous microemulsions, already mentioned above (Lutter et al. 2009; Rojas et al. 2009). Therefore, one can conclude from the cryo-SEM micrographs shown in Fig. 8 that the sample is, indeed, a sugar surfactant-based bicontinuous microemulsion.

Structural properties by SANS

Figure 9 shows the bulk contrast SANS curves of samples D, E, and F. The composition of these samples is given in the section "Methods: Small angle neutron scattering". All three curves show the characteristic broad correlation peak. In the region of this peak the curves were fitted with the Teubner–Strey structure factor:

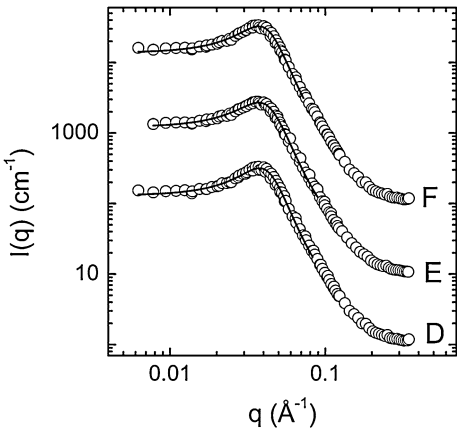

Fig. 9 SANS spectra of bulk contrast samples from the bicontinuous region of the phase diagram shown in Fig. 7. The aqueous phase of the samples was composed of D_2O (D), deuterated buffer solution (E), and DFPase of a concentration of 10 mg/ml in deuterated buffer (F). The curves are spaced for better visualization and fitted with the Teubner–Strey model. Table 2 summarizes the results

$$I(q) = \frac{8\pi c_2 < \eta^2 > /\xi}{a_2 + c_1 q^2 + c_2 q^4} \tag{7}$$

(Teubner and Strey 1987), which results from a Landau–Ginzburg order parameter expansion of the free energy. From the expansion parameters a_2, c_1, c_2, the mean periodicity d of the sponge-like structure:

$$d = 2\pi \left(\frac{1}{2} \left(\frac{a_2}{c_2} \right)^{1/2} - \frac{c_1}{4c_2} \right)^{-1/2}, \tag{8}$$

is obtained. The persistence of the structure, described by the correlation length, ξ, a measure of intermediate range fluctuations, given by:

$$\xi = \left(\frac{1}{2} \left(\frac{a_2}{c_2} \right)^{1/2} + \frac{c_1}{4c_2} \right)^{-1/2} \tag{9}$$

can also be calculated by use of this approach. Table 2 summarizes the composition of the investigated samples and the results of the SANS measurements.

A comparison of the domain size obtained for the three samples indicates no significant change in the microemulsion structure due to the presence of the electrolytes and the enzyme in the aqueous domain. Only the value of the correlation length $\xi = 69.28$ Å decreases slightly by 6% to $\xi = 64.99$ Å for sample F.

Comparison of all the structural parameters calculated on the basis of the SANS data shows that the structure of the bicontinuous region remains stable even for enzyme inclusion in the microemulsion water domain. Furthermore, the correlation length of the amphiphilic film is not changed, which indicates that the enzyme is not embedded into the interface but is preferentially concentrated in the aqueous domain. This finding is in agreement with results for the protein α-chymotrypsin in a reverse droplet AOT–water–heptane microemulsion (Hirai et al. 2002).

DFPase activity measurements using ^{1}H–^{31}P HSCQ NMR spectroscopy

The location of DFPase in the aqueous phase of the microemulsion is a required prerequisite for enzyme activity, because the reaction catalyzed by the enzyme is hydrolytic, but is not a sufficient criterion as it remains unclear if the enzyme maintains its correct folding and catalytic activity in the microemulsion. Therefore, the activity of the enzyme in the microemulsion (composition similar to sample E) was determined. This was achieved by the use of ^{1}H–^{31}P HSCQ NMR spectroscopy (Gäb et al. 2010). This technique enables in-situ observation of nerve agent degradation in complex media, for example microemulsions. Classical ^{1}H NMR spectroscopy cannot be used, because of the high background signals from the surfactant and the cyclohexane. Two microemulsion samples with identical pH of 7.5 were prepared containing 1 mg/g nerve agent sarin (GB). The first microemulsion was spiked with wildtype DFPase and the other sample was left untreated to determine the rate of autohydrolysis. The results are shown in Fig. 10; a distinct acceleration of nerve agent hydrolysis in the sample containing DFPase compared with the sample without enzyme is obvious. In the DFPase sample the nerve agent is completely hydrolyzed within 70 min (using a very small amount of enzyme) whereas in the sample without DFPase only 20% of the nerve agent was degraded at this point. The observation of enzymatic activity in the microemulsion clearly indicates that DFPase can be used in these structured media. However, it should be noted that compared with purely aqueous systems the rate of agent degradation depends not only on the activity of the enzyme

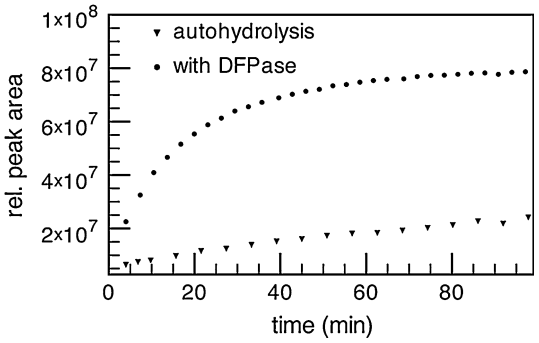

Fig. 10 IMPA (decomposition product of sarin) appearance in the microemulsion with wild type DFPase (*filled circles*) and without enzyme (*filled triangles*)

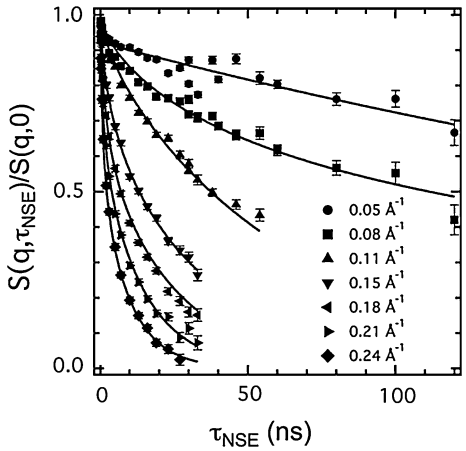

Fig. 11 Normalized intermediate scattering function $S(q, \tau_{NSE})/S(q, 0)$ for the bicontinuous microemulsion in film contrast with a buffered aqueous phase without DFPase (K). *Solid lines* are fits to the model given by Eq. 10

but also on the process of transport of the toxic substrate from the oil to the water phase. This is especially true for more lipophilic agents, leading to a complex interaction of physical transport and chemical catalysis.

Dynamics by NSE

In Fig. 11 the normalized intermediate scattering function $S(q, \tau_{NSE})/S(q, 0)$ for a series of q values in the range 0.05 to 0.24 $Å^{-1}$ are shown, which were obtained from sample K. The composition of this sample is given in the section "Methods: Neutron spin-echo spectroscopy". At the lowest q values measured up to a Fourier time of 120 ns, no complete decay of $S(q, \tau_{NSE})/S(q, 0)$ was observed, whereas the decay of the intermediate scattering function is complete at the highest q value of 0.24 $Å^{-1}$ within the Fourier time window. In Fig. 12 $S(q, \tau_{NSE})/S(q, 0)$ measured for sample M is shown.

Equation 10 was fitted to the data and the results are given as solid lines in Figs. 11 and 12.

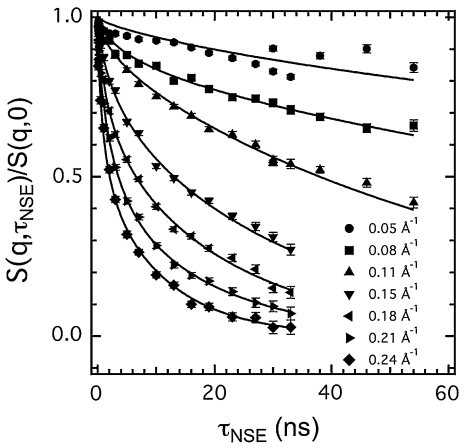

Fig. 12 Normalized intermediate scattering function $S(q, \tau_{NSE})/S(q, 0)$ for the bicontinuous microemulsion in film contrast with a buffered DFPase solution as aqueous phase (Sample M in Table 3). *Solid lines* are fits to the model given by Eq. 10

$$S(q,\tau)/S(q,0) = exp(-\Gamma_{col}\tau)(A + (1-A)exp(-(\Gamma_u\tau)^{\beta}). \quad (10)$$

The model is an empirical approach which combines collective motions of the whole bicontinuous structure and the thermally excited undulations of the amphiphilic interface. The Zilman Granek approach (1996) assumes Zimm dynamics on an ensemble of free-standing membrane plaquettes and is assumed to be applicable to membrane dynamics in bicontinuous microemulsions on short length scales $l \ll \xi$. In this model the normalized intermediate scattering function $S(q, \tau_{NSE})/S(q, 0)$ is given by a stretched exponential function with the stretching exponent $\beta = 2/3$ similar to Zimm polymer dynamics. The decay rate Γ_u describes the relaxation of the thermally excited undulations of the surfactant film and is expected to be proportional to the third power of q. The slope of a respective plot of Γ_u vs. q^3 provides information on the bending elastic constant κ and should follow the form:

$$\Gamma_u = 0.025\gamma_\kappa \left(\frac{k_BT}{\kappa}\right)^{1/2} \frac{k_BT}{\eta} q^3 \quad (11)$$

Here, η is the effective solvent viscosity of the dispersion medium of the membranes and γ_κ is a term with $\gamma_u \rightarrow 1$ for large values of κ.

The bending elasticity constant represents the work required to deform the amphiphilic film from its spontaneous curvature and is of the order of $1k_BT$ for membranes in microemulsions (Strey 1996; Sottmann and Strey 1997). The contribution in Eq. 10 attributed to the collective motion is hydrodynamic in nature and expected to show a q dependence according to $\Gamma_{col} = D_m q^2$, typical for diffusional motion.

In addition to the DLS results for the enzyme solution, Fig. 3 also shows results for this collective breathing mode of the bicontinuous microemulsion sample measured at 20°C by use of DLS. The relaxation rates obtained from the microemulsion sample are smaller than those obtained from the enzyme solution. The result for the microemulsion indicates that hydrodynamic motion exists inside this structure, which can be attributed to thermally excited collective motion of the whole structure on the length and time scales observable with DLS. A value $D_{col} = (1.82 \pm 0.05)\ 10^{-11} m^2/s$ was obtained for the microemulsion sample at 20°C. For a lower temperature the diffusion coefficient will be slightly larger because of slowing down of the collective dynamics caused by the change in viscosity.

Table 3 summarizes the fit results obtained with Eq. 10. In Fig. 13 the obtained values of Γ_{col} are plotted as a function of q^2 for the three samples. From the slope the collective diffusion coefficient D_{col} was obtained. These values compare well with the diffusion coefficient measured by DLS. The relaxation rate Γ_u of the undulation motion is depicted in Fig. 14 and plotted as a function of q^3. The slopes are summarized in Table 3. The bending elasticity was calculated in accordance with Eq. 11. The effective viscosity was given by the mean value of the viscosity of deuterated cyclohexane and D_2O at 15°C, assuming no significant change in the viscosity because of addition of low concentrations of electrolyte, as used in the experiments reported here. The bending elasticities found in the NSE measurements are slightly larger than expected. Within the experimental accuracy no difference was found for microemulsions with and without enzyme inside the aqueous phase. The presence of the enzyme does not change the interfacial curvature, which shows that the enzyme is preferentially localized inside the aqueous phase and does not alter the structure or dynamics of the microemulsion's internal interface. The microemulsion only produces the necessary hydrophobic and hydrophilic compartments to solubilize the enzyme and the water insoluble substrate.

Conclusion

Several scattering techniques were used to determine the structure of diisopropyl fluorophosphatase in aqueous

Table 3 Results for the collective and undulation dynamics of a bicontinuous sample with different compositions of the aqueous domain

Sample	c (mg/ml)	D_m (10^{-7} cm^2/s)	κ (k_BT)
K	0	1.75 ± 0.09	1.6 ± 0.2
L	5.0	1.66 ± 0.06	1.4 ± 0.1
M	10.0	1.60 ± 0.05	1.6 ± 0.2

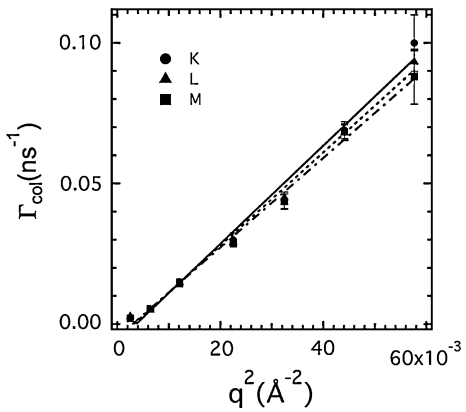

Fig. 13 Relaxation rate Γ_{col} of the undulation motion obtained from fits according to Eq. 10 for three microemulsion samples. The *lines* are linear fits and the results are summarized in Table 3

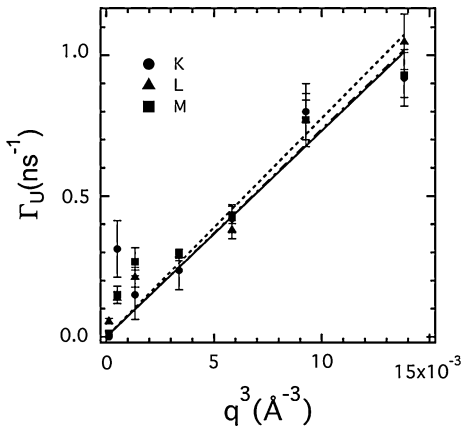

Fig. 14 Relaxation rate Γ_u of the undulation motion obtained from fits according to Eq. 10 for three microemulsion samples. The *lines* are linear fits and the results are summarized in Table 3

buffer at concentrations up to 10 mg/ml. SANS, DLS, and NSE measurements confirm the approximately globular structure of the enzyme in its native state, and results are in good agreement with those from protein crystallography. A diffusion coefficient of $D_m = (6.52 \pm 0.21) \times 10^{-7}$ cm^2/s and a hydrodynamic radius of $R_h = 2.34$ nm were determined by DLS. Additional hydrodynamic model calculations result in a diffusion coefficient of $D = 6.55 \times 10^{-7}$ cm^2/s, which is in very good agreement with the experimental results. NSE data give an effective diffusion coefficient corresponding to the light scattering value and to the calculated data at low q values. The increase of D_{eff} at larger q can be attributed to the contribution of internal modes close to the form factor minimum.

In the quaternary system cyclohexane–water–$C_{8/10}G_{1.3}$–pentanol bicontinuous microemulsions were investigated as model systems for sugar surfactant-based carrier media for enzymatic decontamination of toxic organophosphates. The bicontinuous region was characterized with cryo-SEM imaging and SANS. A mean domain size within the region of 15–16 nm and a correlation length of 6–7 nm were found. The structure remains unchanged in the presence of DFPase confined in the aqueous domain. NSE measurements gave a bending elastic constant of the amphiphilic interface of $\sim 1.5\ k_BT$. From these results we conclude that the presence of DFPase does not change the properties of the surfactant film, which separates the enzyme containing water phase from the oil phase solubilizing the substrate.

Furthermore, ^{1}H–^{31}P HSCQ NMR spectroscopy was used to confirm the activity of DFPase inside the aqueous phase of the microemulsion.

The experimental results demonstrate that enzymatic hydrolysis of sarin can be achieved in the complex environment of a microemulsion. The DFPase does not accumulate in the interfacial layer of the microemulsion, which indicates that, because of the limited solubility of the nerve agents in water, concentration gradient-driven transport towards the aqueous phase is essential for the reaction. In this picture the oil phase serves as the reservoir of the nerve agent, extracted from a contaminated hydrophobically coated surface. In further investigations the reaction mechanism, e.g. the reaction rate, will be tested using bicontinuous microemulsions of different oil-to-water ratios and the decontamination process could be optimized by tuning the interface for faster passage of the substrate.

In summary, the reported results reveal that sugar surfactant-based bicontinuous microemulsions are "mild" reaction media for enzymatic decontamination. They overcome the problem of solubilization of the hydrophobic substrate. Hence, they are promising environmentally compatible compartmentalized reaction media providing interesting properties for biotechnological applications in general.

Acknowledgments J.G. and M.M.B. were supported by the German Ministry of Defense under contract E/UR3G/6G115/6A801. T.H., R.S., C.S. also were financed by the German Ministry of Defense (Contracts E/E590/9Z004/5F159 and E/E590/8Z002/4F170). The SANS experiments were supported by the European Union through the NMI3 program. We are grateful to the Laboratoire Léon Brillouin and the Jülich Center for Neutron Scattering at the FRM II for providing beamtime.

References

Arriaga LR, Lopez-Montero I, Monroy F, Gil GO, Farago B, Hellweg T (2009a) Stiffening effect of cholesterol on disordered lipid phases: a combined NSE + DLS analysis of the bending elasticity of large unilamellar vesicles based on POPC. Bipohys J 96:3629–3637

Arriaga LR, Lopez-Montero I, Monroy F, Gil GO, Farago B, Hellweg T (2009b) Fluctuation dynamics of rigid vesicles: frustration of regular bulk dissipation into a sub-diffusive relaxation. Phys Rev E 80:031908

Arriaga LR, Rodriguez-Garcia R, Lopez-Montero I, Farago B, Hellweg T, Monroy F (2010) Dissipative curvature fluctuations in bilayer vesicles: coexistence of pure-bending and hybrid curvature-compression modes. Euro Phys J E 31:105–115

Aveyard R, Binks BP, Fletcher PDI, Buscall R, Davies S (1998) Surface and colloid chemistry of systems containing pure sugar surfactants. Langmuir 14:4699–4709

Baier J, Koetz J, Kosmella S, Tiersch B, Rehage H (2007) Polyelectrolyte-modified inverse microemulsions and their use as templates for the formation of magnetite nanoparticles. J Phys Chem B 111(29):8612–8618

Bargeron CB (1974) Measurement of continuous distribution of spherical particles by intensity correlation spectroscopy: analysis by cumulants. J Chem Phys 61(5):2134–2138

Biehl R, Hoffmann B, Monkenbusch M, Falus P, Prevost S, Merkel R, Richter D (2008) Direct observation of correlated interdomain motion in alcohol dehydrogenase. Phys Rev Lett 101:138102-1–138102-4

Biswas R, Das AR, Pradhan T, Touraud D, Kunz W, Mahiuddin S (2008) Spectroscopic studies of catanionic reverse microemulsion: correlation with the superactivity of horseradish peroxidase enzyme in a restricted environment. J Phys Chem B 112(21): 6620–6628

Blum MM, Löhr F, Richardt A, Rüterjans H, Chen JCH (2006) Binding of a designed substrate analogue to diisopropyl fluorophosphatase: implications for the phosphotriesterase mechanism. J Am Chem Soc 128:12750–12757

Blum MM, Mustyakimov M, Rüterjans H, Kehe K, Schoenborn BP, Langan P, Chen JCH (2009) Rapid determination of hydrogen positions and protonation states of diisopropyl fluorophosphatase by joint neutron and X-Ray diffraction refinement. PNAS 106:713–718

Brûlet A, Lairez D, Lapp A, Cotton JP (2007) Improvement of data treatment in small-angle neutron scattering. J Appl Cryst 40:165–177

Bu Z, Biehl R, Monkenbusch M, Richter D, Callaway DJE (2005) Coupled protein domain motion in Taq polymerase revealed by neutron spin-echo spectroscopy. PNAS 102(49):17646–17651

Burauer S, Sachert T, Sottmann T, Strey R (1999) On microemulsion phase behavior and monomeric solubility of surfactant. PCCP 1:4299–4306

Burchard W, Richtering W (1989) Dynamic light scattering from polymer solutions. Progr Colloid Polymer Sci 80:151–163

Carnahan NF, Starling KE (1969) Equation of state for noninteracting rigid spheres. J Chem Phys 51(2):635–636

Coeur CL, Longeville S (2008) Microscopic protein diffusion at high concentration by neutron spin-echo spectroscopy. Chem Phys 345:298–304

Cotton JP (1991) Initial data treatment. In: Lindner P, Zemb T (eds), Neutron, X-ray and light scattering. Elsevier Science Publishers B.V.

Doster W, Longeville S (2007) Microscopic diffusion and hydrodynamic interactions of hemoglobin in red blood cells. Biophys J 93:1360–1368

Endo H, Mihailescu M, Monkenbusch M, Allgaier J, Gompper G, Richter D, Jakobs B, Strey R, Grillo I (2001) Effect of amphiphilic block copolymers on the structure and phase behavior of oil-water-surfactant mixtures. J Chem Phys 115(1):580–600

Farago B, Gradzielski M (2001) The effect of the charge density of microemulsion droplets on the bending elasticity of their amphiphilic film. J Chem Phys 114(22):10105–10122

Farago B, Richter D, Huang JS, Safran SA, Milner ST (1990) Shape and size fluctuations of microemulsion droplets: the role of cosurfactant. Phys Rev Lett 65(26):3348–3351

Farago B, Monkenbusch M, Goecking KD, Richter D, Huang JS (1995) Dynamics of microemulsions as seen by neutron spin echo. Physica B 213 & 214:712–717

Gäb J, Melzer M, Kehe K, Wellert S, Hellweg T, Blum MM (2010) Monitoring the hydrolysis of toxic organo-phosphates and -phosphonates by diisopropyl fluorophosphatase from Loligo vulgaris by 1D ^{1}H-^{3}1P-HSQC NMR spectroscopy in aqueous solution and bicontinuous microemulsions. Anal Bioanal Chem 396:1213–1221

Garcia Bernal JM, Garcia de la Torre J (1980) Transport properties and hydrodynamic centers of rigid macromolecules with arbitrary shapes. Biopolymers 19:751–766

Garcia de la Torre J, Bloomfield VA (1977) Hydrodynamic properties of macromolecular complexes. 1. Translation. Biopolymers 16:1747–1763

Garcia de la Torre J, Bloomfield VA (1981) Hydrodynamic properties of complex, rigid biological macromolecules: Theory and application. Quarterly Rev Biophys 14:81–139

Garcia de la Torre J, Huertas ML, Carrasco B (2000) Calculation of hydrodynamic properties of globular proteins from their atomic-level structure. Biophys J 78(2):719–730

Glatter O, Orthaber D, Stradner A, Scherf G, Fanun M, Garti N, Clement V, Leser ME (2001) Sugar-ester nonionic microemulsion: structural characterization. J Coll Inter Sci 241:215–225

Hartleib J, Rüterjans H (2001) High-yield expression, purification, and characterization of the recombinant diisopropylfluorophosphatase from Loligo vulgaris. Prot Expr Purif 21(1):210–219

Helfrich W (1973) Elastic properties of lipid bilayers: theory and possible experiments. Z Naturforschung 28c:693–703

Hellweg T (2002) Phase structures of microemulsions. Curr Opin Colloid Interface Sci 7:50–56

Hellweg T, von Klitzing R (2000) Structural changes and complex dynamics in the single phase region of a dodecane/$C_{12}E_5$/Water microemulsion: a dynamic light scattering study. Physica A 283(3–4):349–358

Hellweg T, Hinssen H, Eimer W (1993) A dynamic light scattering study on the two proteolytic fragments of gelsolin. Biophys J 65:799–805

Hellweg T, Eimer W, Krahn E, Schneider K, Müller A (1997) Hydrodynamic properties of nitrogenase–the MoFe protein from Azotobacter vinelandii studied by dynamic light scattering and hydrodynamic modelling. Biochim Biophys Acta 1337:311–318

Hellweg T, Brûlet A, Sottmann T (2000) Dynamics in an oil-continuous droplet microemulsions as seen by quasielastic scattering techniques. Phys Chem Chem Phys 2(22):5168–5174

Hellweg T, Gradzielski M, Farago B, Langevin D (2001) Shape fluctuation of microemulsion droplets: a neutron spin-echo study. Colloids Surfaces A 183–185:159–169

Hirai M, Hirai RK, Iwase H, Arai S, Mitsuya S, Takeda T, Seto H, Nagao M (1999) Dynamics of w/o AOT microemulsion studied by neutron spin echo. J Phys Chem Solids 60(8–9): 1359–1361

Hirai M, Hirai RK, Iwase v, Hayakawa T, Kawabata Y, Takeda T (2002) Effect of proteins on dynamics of water-in-oil AOT microemulsion. Appl Phys A 74:S1254–S1256

Holderer O, Frielinghaus H, Byelov D, Monkenbusch M, Allgaier J, Richter D (2005) Dynamic properties of microemulsins modified with homopolymers and diblock copolymers: the determination of bending moduli and renormalization effects. J Chem Phys 122:094908/1–094908/8

Holmberg K (2001) Natural surfactants. Curr Opin Colloid Interface Sci 6:148–159

Hoskin FCG (1971) Diisopropylphosphorofluoridate and tabun: enzymatic hydrolysis and nerve function. Sci Agric 172:1243–1245

Hoskin FCG, Roush AH (1982) Hydrolysis of nerve gas by squid-type diisopropyl phosphorofluoridate hydrolyzing enzyme on agarose resin. Sci Agric 215:1255–1257

Huang JS, Milner ST, Farago B, Richter D (1987) Study of dynamics of microemulsion droplets by neutron spin-echo spectroscopy. Phys Rev Lett 59(22):2600–2603

Iwanaga T, Suzuki M, Kunieda H (1998) Effect of added salts or polyols on the liquid crystalline structures of polyoxyethylene-type nonionic surfactants. Langmuir 14:5775–5781

Jahn W, Strey R (1988) Microstructure of microemulsions by freeze-fracture electron-microscopy. J Phys Chem 92:2294–2301, Keine Kopie

Kahlweit M et al (1987) How to study microemulsions. J Colloid Interface Sci 118(2):436–453

Kahlweit M, Strey R (1985) Phasenverhalten ternärer Systeme des Typs H_2O-Öl-nichtionisches Amphiphil (Mikroemulsionen). Angew Chem 97:655–669

Kawabata Y, Seto H, Nagao M, Takeda T (2007) Pressure effects on bending elasticities of surfactant monolayers in a ternary microemulsion composed of aerosol-OT/D_2O/decane. J Chem Phys 127:044705-1–044705-9

Kirkwood JG (1949) The statistical mechanical theory of irreversible processes in solutions of flexible macromolecules. Recueil Trav Chim 68:649–660

Koeper I, Bellissent-Funel MC (2000) Hindered protein dynamics in the presence of a cryoprotecting agent. Appl Phys A 74:S1257–S1259

Koepke J, Scharff EI, Lücke C (2003) Statistical analysis of crystallographic data obtained from squid ganglion DFPase at 0.85 Å resolution. Acta Crystallographica D 59:1744–1754

Kohlbrecher J (2008) SASfit: A program for fitting simple structural models to small angle scattering data. Paul Scherrer Institut, Laboratory for Neutron Scattering, CH-5232 Villigen, Switzerland

Komves C, Osborne D, Russell AJ (1994) Degredation of pesticides in a contiuous-flow 2-phase microemulsion reactor. Biotechnol Prog 10(3):340–343

Koppel DE (1972) Analysis of macromolecular polydispersity in intensity correlation spectroscopy: the method of cumulants. J Chem Phys 57(11):4814–4820

Larsson KM, Adlercreutz P, Mattiasson B, Olsson U (1991) Enzyme catalysis in uni- and bi-continuous microemulsions: dependence of kinetics on substrate partitioning. J Chem Soc Faraday Trans 87:465–471

Lee KM, Biellmann JF (1987) Enzyme and organic solvents: horse liver alcohol dehydrogenase in non-ionic microemulsion: stability and activity. FEBS Lett 223(1):33–36

Lutter S, Koetz J, Tiersch B, Kosmella S (2009) Polymer-modified bicontinuous microemulsions used as a template for the formation of nanorods. J Dispersion Sci Technol 30:745–752

Mihailescu M, Monkenbusch M, Endo H, Allgaier J, Gompper G, Richter D, Jakobs B, Sottmann T, Farago B (2001) Dynamics of bicontinuous microemulsion phases with and without amphiphilic block-copolymers. J Chem Phys 115(20):9563–9577

Milner ST, Safran SA (1987) Dynamical fluctuations of droplet microemulsions and vesicles. Phys Rev A 36(9):4371–4379

Möller A, Lang P, Findenegg GH, Keiderling U (1998) Location of butanol in mixed micelles with alkyl glucosides studied by SANS. J Phys Chem B 102(45):8958–8964

Monkenbusch M (1997) The Jülich neutron spin echo spectrometer. Neutron News 8(1):25

Monkenbusch M, Schatzler R, Richter D (1997) The Julich neutron spin-echo spectrometer–design and performanc. Nucl Instrum Methods Phys Res Sect A 399(2–3):301–323

Pedersen JS (1997) Analysis of small-angle scattering data from colloids and polymer solutions: modeling and least-square fitting. Adv Coll Inter Sci 70:171–210

Provencher SW (1982a) A constrained regularization method for inverting data represented by linear algebraic or integral equations. Comput Phys Com 27:213–217

Provencher SW (1982b) Contin: a general purpose constrained regularization program for inverting noisy linear algebraic and integral equations. Comput Phys Com 27:229–242

Richardt A, Blum MM (2008) Decontamination of Warfare Agents Wiley-VCH, Weinheim ISBN-10:3-527-31756-2

Riseman J, Kirkwood JG (1950) The intrinsic viscosity, translational and rotatory diffusion constants of rod-like macromolecules in solution. J Chem Phys 18(4):512–516

Rojas O, Koetz J, Kosmella S, Tiersch B, Kramer M, Wacker P (2009) Structural studies of ionic liquid-modified microemulsions. J Coll Interf Sci 33:782–790

Safran SA (1999) Curvature elasticity of thin films. Adv Phys 48(4):395–448 Review

Scharff EI, Koepke J, Fritzsch G, Lücke C, Rüterjans H (2001) Crystal structure of diisopropylfluorophosphatase from Loligo vulgaris. Structure 9:493–502

Sottmann T, Strey R (1997) Ultralow interfacial tensions in water-n-alkane-surfactant systems. J Chem Phys 106(20):8606–8615

Stamatis H, Xenakis A, Kolisis FN (1999) Bioorganic reactions in microemulsions: the case of lipases. Biotechnl Adv 17:293–318

Stradner A, Glatter O, Schurtenberger P (2000) A hexanol-induced sphere-toflexible cylinder transition in aqueous alkyl polyglucoside solutions. Langmuir 16(12):5354–5364

Strey R (1994) Microemulsion microstructure and interfacial curvature. Coll Polymer Sci 272:1005–1019

Strey R (1996) Phase behavior and interfacial curvature in water-oil-surfactant systems. Curr Opin Colloid Interface Sci 1:402–410

Stubenrauch C (2001) Sugar surfactants–aggregation, interfacial, and adsorption phenomena. Curr Opin Colloid Interface Sci 6:160–170

Teubner M, Strey R (1987) Origin of the scattering peak in microemulsions. J Chem Phys 87(5):3195–3200

Wellert S, Karg M, Imhof H, Steppin A, Altmann HJ, Dolle M, Richardt A, Tiersch B, Koetz J, Lapp A, Hellweg T (2008) Structure of Biodiesel based bicontinuous microemulsions for environmentally compatible decontamination as seen by small angle neutron scattering and freeze fracture electron microscopy. J Colloid Interf Sci 325:250–258

Wood K, Caronna C, Fouquet P, Häussler W, Natali F, Ollivier J, Orecchini A, Plazanet M, Zaccai G (2008) A benchmark for protein dynamics: Ribonuclease as measured by neutron scattering in a large wavevector-energy transfer range. Chem Phys 345:305–314

Zilman AG, Granek R (1996) Undulations and dynamic structure factor of membranes. Phys Rev Lett 77:4788–4791

Zouni A, Kern J, Frank J, Hellweg T, Behlke J, Saenger W, Irrgang KD (2005) Size determination of cyanobacterial and higher plant photosystem II by gel permeation chromatography, light scattering, and ultracentrifugation. Biochem 44(11):4572–4581